Acta Biomaterialia xxx (xxxx) xxx



Contents lists available at ScienceDirect

## Acta Biomaterialia

journal homepage: www.elsevier.com/locate/actbio



Full length article

# Humidity mediated performance and material properties of orb weaving spider adhesive droplets

Brent D. Opell\*, Hannah Mae Elmore, Mary L. Hendricks

Department of Biological Sciences, Virginia Tech Blacksburg, VA 24061 United States

## ARTICLE INFO

Article history: Received 16 February 2021 Revised 5 June 2021 Accepted 8 June 2021 Available online xxx

Keywords:
Bioadhesive
Biomechanics
Elastic modulus
Environmental responsiveness
Soft matter
Toughness

#### ABSTRACT

Capture thread glue droplets retain insects that strike an orb web and are key to the success of over 4,600 described spider species. Each droplet is a self-assembling adhesive system whose emergent biomechanical properties are centered on its viscoelastic, protein core. This bioadhesive is dependent on its surrounding hygroscopic aqueous layer for hydration and chemical conditioning. Consequently, a droplet's water content and adhesive performance track environmental humidity. We tested the hypothesis that natural selection has tuned a droplet's adhesive performance and material properties to a species' foraging humidity. At 55% relative humidity (RH) the adhesive properties of 12 species ranged from that of PEG-based hydrogels to that of silicone rubber, exhibiting a 1088-fold inter-specific difference in stiffness (0.02-21.76 MPa) and a 147-fold difference in toughness (0.14-20.51 MJ/m³). When tested over a 70% RH range, droplet extension lengths per protein core volume peaked at lower humidities in species from exposed, low humidity habitats, and at higher humidities in nocturnal species and those found in humid habitats. However, at the RH's where these species' maximum extension per protein volume indices were observed, the stiffness of most species' adhesive did not differ, documenting that selection has tuned elastic modulus by adjusting droplet hygroscopicity. This inverse relationship between droplet hygroscopicity and a species' foraging humidity ensures optimal adhesive stiffness. By characterizing the humidity responsiveness and properties of orb spider glue droplets, our study also profiles the range of its biomimetic potential.

## Statement of significance

Over 4,600 described species of orb weaving spider rely on tiny glue droplets in their webs to retain insect that the web intercepts. The aqueous layer that covers each droplet's core allows this adhesive to remain pliable and to stretch as an insect struggles to escape. The aqueous solution also attracts water from the air, causing the glue droplet's performance to change with humidity. By characterizing the droplet extensions and adhesive material properties of twelve species at relative humidities between of 20 and 90%, this study examined how this unique adhesive system responds to its environment and how it is tuned to the humidity of a species' habitat.

© 2021 Acta Materialia Inc. Published by Elsevier Ltd. All rights reserved.

## 1. Introduction

Soft matter is often characterized by "complex emergent behavior, such as spontaneous pattern formation, self-assembly, and a large response to small external stimuli" [1]. Few materials illustrate this better than the viscous prey capture thread of a spider's orb web. This thread is deposited on radial threads as a single spiral extending from the web's frame threads to its hub (Fig. 1A).

\* Corresponding author.

E-mail address: bopell@vt.edu (B.D. Opell).

Like the web's non-adhesive threads, the capture thread's supporting flagelliform fibers and its viscoelastic core (Figs. 1B-C) [2,3] are products of the spidroin gene family [4,5]. However, consistent with their respective roles in prey capture, the material properties of these web elements differ. The stiff major ampullate fibers that form the radial and frame threads absorb and dissipate the force of prey impact [6,7]. In contrast, the capture thread's more extensible flagelliform fibers and it's even more pliable adhesive retain an intercepted insect until a sider can locate, run to, and subdue its prey [8].

https://doi.org/10.1016/j.actbio.2021.06.017

1742-7061/© 2021 Acta Materialia Inc. Published by Elsevier Ltd. All rights reserved.

Acta Biomaterialia xxx (xxxx) xxx

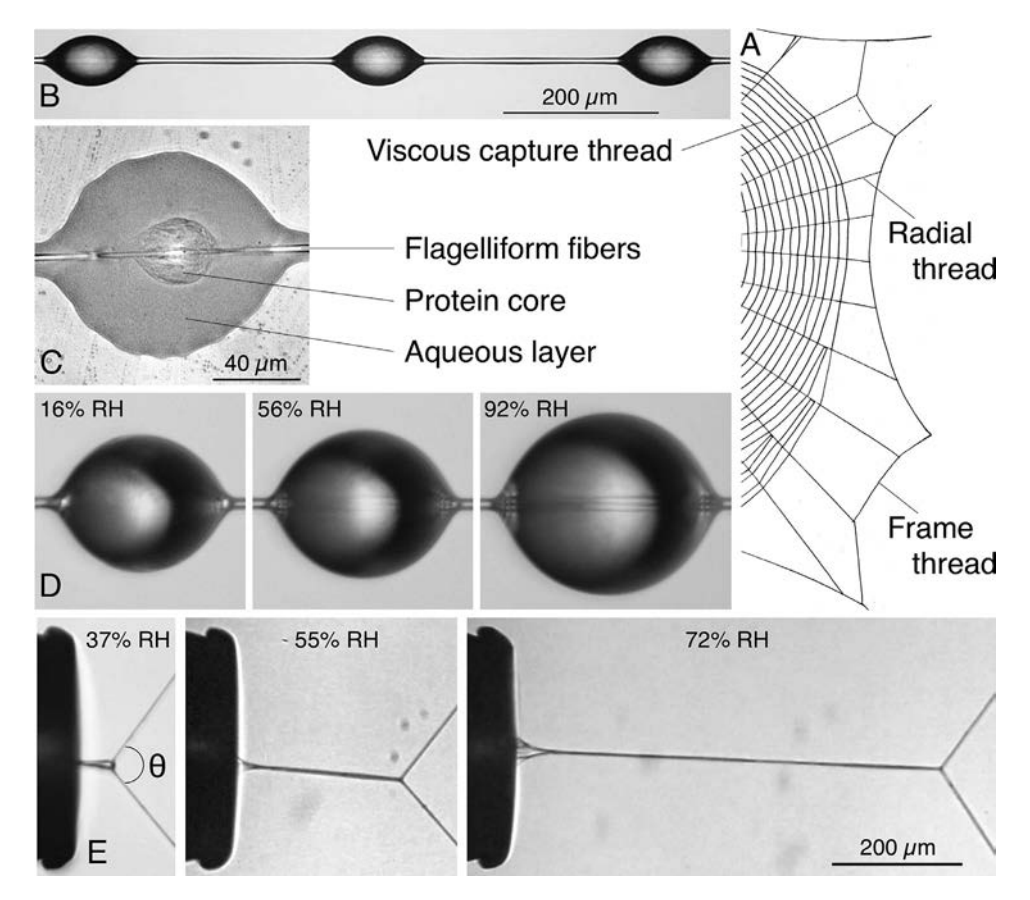


**Fig. 1.** Orb webs and their prey capture threads. A. Orb web frame, radial, and prey capture threads identified. B. *Argiope aurantia* capture thread span. C. Flattened *A. aurantia* droplet revealing its supporting flagelliform fiber pair, outer aqueous layer, and inner protein core. D. The same *A. aurantia* droplet photographed at three relative humidities, illustrating how absorbed atmospheric moisture increases droplet volume. E. Droplets of the same *Neoscona crucifera* individual extended to the point of pull-off at three relative humidities (RH).

Three spinning spigots on each of a spider's paired posterior lateral spinnerets produce a capture thread [9–11]. As a protein fiber emerges from the flagelliform spigot, it is coated with aqueous solution from two flanking aggregate gland spigots. The coated fibers from the two spinnerets merge to form a single strand. Plateau-Rayleigh instability quickly reconfigures this strand's initially cylindrical aggregate coat into a series of regularly spaced droplets (Fig. 1B) [12]. Within each droplet a core forms (Fig. 1C). This has often been termed a glycoprotein core to reflect its earliest identified major component [3,13]. However, phosphorylated proteins have recently been identified in the cores of the araneoid family Theridiidae [14]. Therefore, we refer to this material simply as protein. This material interacts with other droplet components to adhere a droplet to a surface.

After these protein cores coalesce an aqueous layer comprised of inorganic salts, organic low molecular mass compounds (LMMCs), and amorphous proteins covers the droplet core and flagelliform fibers, both within and between droplets [15-17]. This aqueous layer hydrates these thread components, maintains their extensibilities, and solvates and conditions the protein core [18-21]. Therefore, droplet adhesion is likely the result of interaction among the protein core, aqueous layer components, and a surface. Moreover, largely as a result of its LMMCs, the aqueous layer confers thread hygroscopicity, causing both droplet volume and adhesive performance to respond to changes in environmental humidity (Figs. 1D and 1E) [22-25]. An additional reconfiguration of a capture thread occurs when force is applied to droplets that have adhered to a surface. The thread's flagelliform fibers and its more extensible core protein both extend to assume a suspension bridge

configuration [26]. This robust adhesion relies on the synergistic interplay of flagelliform fibers and core protein to sum the adhesive forces of multiple thread droplets [27,28] and dissipate the forces of an insect's struggles [29]. Thus, in contrast with the adhesives of barnacles and mussels, which form rigid anchors [30], orb spider adhesive functions as a dynamic adhesive delivery system.

The appearance of viscous prey capture threads is associated with the success of the seven orb weaving Araneoidea families (in order of decreasing number of species, Araneidae, Tetragnathidae, Anapidae, Mysmenidae, Theridiosomatidae, Symphytognathidae, and Synaphridae), which include over 4,600 described species in 329 genera [31,32]. An additional 2,800 described species in the families Theridiidae and Nesticidae continue to include aggregate adhesive on the gumfoot lines of their derive webs [33]. Some members of the family Linyphiidae, which is comprised of 4,700 species, also produce aggregate adhesive, although the number of species that do this is poorly documented, as is the contribution of this glue to prey capture [34-36].

Because orb weavers occupy habitats ranging from arid grass-lands to rainforests, a crucial question that underpins an increasing number of studies of these capture threads is "How have the properties and performance of droplets evolved to adapt a species to the humidity regime of its habitat?" The broad answer to this question has been framed by studies showing that the adhesion and extension of a species' glue droplets and thread are greatest at its foraging humidity [25,29,37], that, at this foraging humidity, core material viscosity of diverse species is remarkably similar [23], and that differences in the composition and concentration of the aqueous layer's LMMCs are largely responsible for tuning a

Acta Biomaterialia xxx (xxxx) xxx

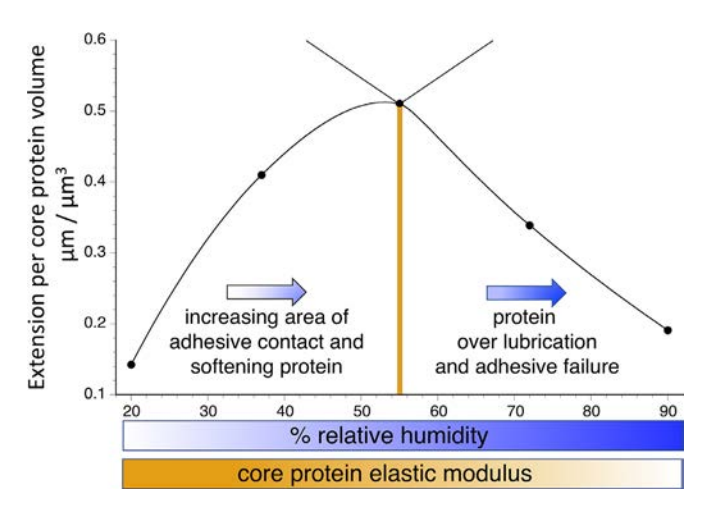


**Fig. 2.** Model of glue droplet extension as exhibited by *L. venusta*. As humidity increases, droplets absorb more atmospheric moisture, causing their protein cores to soften and the protein's elastic modulus to decrease. This initially results in increased area of adhesive contact and decreased resistance to protein extension. However, when the protein becomes oversaturated with water, which, in this species occurs at 55% RH, droplets pull-off at progressively shorter lengths.

thread's performance to a species' foraging humidity. This is documented by differences in both the kinds and percentages of LMMCs in the aqueous layers of seven orb weaving species' glue droplets [16,25].

Optimum droplet performance is achieved when adhesive viscosity is low enough to allow spreading, which is necessary to establish adhesive contact, but adhesive cohesion remains high enough to maintain the integrity of an extending core material filament (Fig. 1E) [23]. A study comparing insect retention times by simple orb web capture thread arrays documented that humidity impacts prey retention time and that the material properties of both a thread's core material and its flagelliform fibers contribute to retention time [38]. Droplet core material elastic (Young's) modulus was also a critical component of a biomechanical model that explained the dynamics of capture thread suspension bridges [28]. As humidity increases and a glue droplet absorbs atmospheric moisture the volume of its core increases and this material softens, allowing the droplet's adhesive to both establish a greater surface area of adhesive contact and to extend a greater distance before pull-off (Fig. 1E, Fig. 2). However, at some point, the core absorbs excess water and becomes over lubricated resulting in adhesive failure and shorter droplet extension lengths (Fig. 2) [29,37].

Thus, we currently view orb web glue droplets as performing optimally at a species' foraging humidity because, at this humidity, a droplet's hygroscopic compounds attract an amount of water sufficient to cause the core protein to flatten and establish adhesive contact while ensuring that it remains stiff enough during extension to contribute adhesive force to a capture thread span. The objective of our study was to test this hypothesis in the context of humidities that twelve orb weaving species experience. We did this by characterizing these species' foraging humidities to ensure that our results were correctly interpreted and by comparing the performance and material properties of their adhesive droplets over a 70% relative humidity (RH) range. At each of five humidities we determined the extension per adhesive volume and the elastic modulus of these species' protein cores. At 55% RH we also determined protein toughness. The hypothesis predicts that, when compared at each species' foraging humidity, the elastic moduli of their core proteins will be more similar than when compared at a common, mid-range humidity. We believe that this perspective will increase the understanding of how orb weaving spider capture threads operate under natural conditions and how the evolution

of this bioadhesive has contributed to the great diversity of this widely distributed group of spiders. The resulting profile of their core proteins' material properties may also make the biomimetic potential of this natural adhesive more attractive.

We characterized the properties of these glue droplets' small protein cores while contained within their aqueous layers from images of suspended and flattened glue droplets (Figs. 1B-D) and from videos of droplets that were extended to pull-off (Fig. 1E). Knowing the diameter and elastic modulus of a species' flagelliform fibers, we used the deflection angle of the droplet's support line during extension to compute the force on the droplet's protein filament and used this and the length of the filament to construct true stress - true strain curves from which core material elastic modulus and toughness were derived. This was possible only at the 55% RH test humidity because this humidity was similar to that at which flagelliform fiber properties were determined. Therefore, we used a species' droplet extension per protein volume index to adjust the elastic modulus of its core protein determined at 55% RH to the four other test humidities.

#### 2. Materials and methods

#### 2.1. Collecting threads and preparing droplets for testing

We used rings or rectangular frames surfaced with doubled sided tape to collected sectors of orb webs spun by 11-14 adult female spiders of twelve species (Fig. 3; pruned tree based on [39]) found in habitats near Blacksburg, VA. Spiders were not collected, as the species and maturity of each could be easily identified in the field. Consequently, sample collecting had no more effect on a spider than did a rainy day that damaged its web. Voucher specimens of each species are deposited in the Smithsonian Institution's Natural History Museum. Web samples were kept in closed containers at approximately 50% RH until thread samples were prepared for testing. Web samples from webs spun by nocturnal species were collected in the evening and tested by 16:00 on the following day. Samples of other species were collected in the early morning and tested by 16:00 on the same day. After transferring an individual's capture thread strand to supports of a microscope slide thread sampler, we isolated a focal droplet at the center of the 4800 µm thread span to ensure that a probe used to extend droplets contacted only a single droplet [37,40,41].

#### 2.2. Assigning foraging humidity categories

The habitats and activity patterns of these species expose them to different humidities as they forage (Fig. 4) and allow us to assign species to three habitat humidity groups: 1. Exposed, weedy vegetation characterized by low late morning and afternoon humidities, 2. Forest edge habitats characterized by intermediate daytime humidity, and 3. Deep forest, adjacent to water, and nocturnal web builders, all of which experience high humidity when foraging. Humidity recordings from these habitats document these differences in foraging humidities (Fig. 4). Populations of V. arenata and L. cornutus that we studied construct webs soon after sunset, monitor them from a position at the hub during the night and continue to use webs during the following day unless webs are extensively damaged. However, during daylight hours members of both species monitor their webs form protected sites adjacent to their webs. Verrucosa arenata typically selects a crevice or hole, whereas N. crucifera usually rests in vegetation. Consequently, both species experience a wider range of foraging humidities than most species, although this is dominated by high humidity.

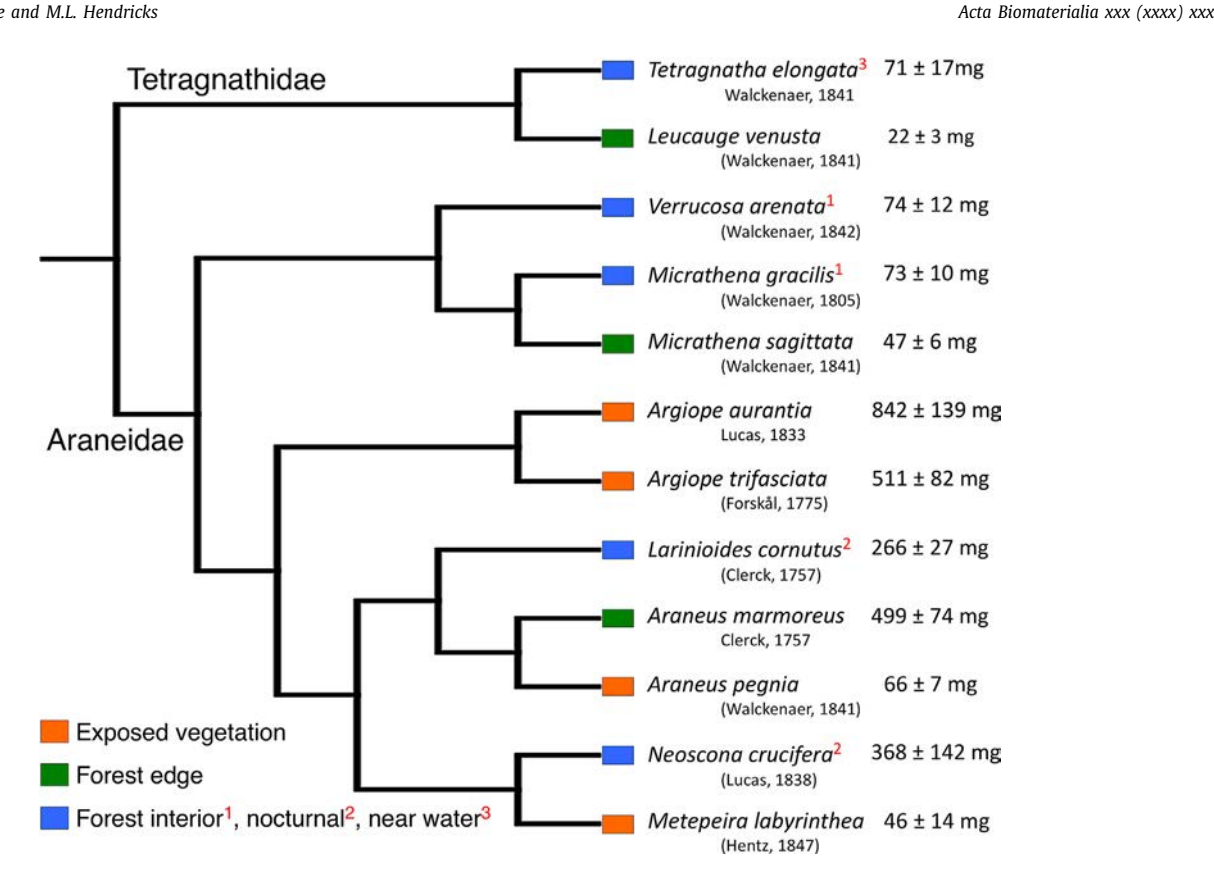


Fig. 3. Relationships among the twelve study species, their habitats, and adult female masses. Phylogeny based on [38], with T. elongate substituted for its congener T. versicolor. Spider masses are from [25,43].

#### 2.3. Establishing temperature and humidity

The thread sampler was placed in a glass covered observation chamber that rested on the mechanical stage of a Mitutoyo FS60 inspection microscope (Mitutoyo America Corp., Aurora IL, USA). Temperature was maintained at 23°C by a thermostat controlled Peltier thermocouple attached to the aluminum chamber's wall. We monitored chamber humidity with a Fisher Scientific® Instant Digital Hygrometer, whose tip extended through the chamber wall. We established 20%, 37%, 55%, 72%, and 90% RH test conditions by using a small dish of silica gel desiccant to lower humidity and a piece of distilled water moistened Kimwipe® to raise humidity. Small adjustments to humidity were made by drawing room air into the chamber through a side port to lower humidity and by blowing gently into a tube that connected to the chamber by a cylinder packed with distilled water saturated cotton to increase humidity. These methods tightly controlled humidity, as shown in Table S1.

#### 2.4. Determining droplet and core protein volumes

Amorphous proteins are present in the aqueous layer [15], but the degree to which these proteins contribute to a droplet's extending protein filament is unknown. Therefore, because we could not quantify these proteins, we base our calculations of a droplet's protein core volume on the protein core that we could visualize. To do this we photographed three droplets of a suspended thread strand from each individual's web sample at each of the five test humidities. Droplets were then flattened by releasing an alcohol cleaned glass coverslip onto the thread from a magnetically triggered device contained within the observation chamber, ensuring that the humidity remained unchanged during this procedure. We then identified and photographed the same three droplets; all of this being done without opening the observation chamber and within one or two minutes after flattening occurred. This timing was consistent with that used to adhere droplets prior to extension. In addition to ensuring consistency between procedures, this minimized post-contact protein adhesive creep.

Using Image J [42] we measured the length (DL, dimension parallel to the thread's support lines) and width (DW) of each suspended droplet (Fig. 1D) and computed its volume (DV) using the following formula [43].

$$DV = \frac{2\pi \ x \ DW^2 \ x \ DL}{15}$$

We next measured the surface area of the flattened droplets and of their protein cores (Fig. 1C). Dividing droplet volume by droplet surface area yields flattened droplet thickness, which we multiplied by protein surface area to determine protein core volume. From these three droplet's measurements we computed mean individual- and humidity-specific protein core -to-droplet volume ratios. These ratios permitted us to infer the volume of protein within an individual's extended droplets without altering droplets prior to extension. Protein volumes of the twelve species are provided in Tables S3 - S14.

## 2.5. Extending droplets

A single droplet from each A. aurantia and N. crucifera web was extended at each RH. For all other species we extended two droplets per web sample at each RH and in statistical analyses used the mean values determined from these two extensions to determine an individual's adhesive properties at each RH. A steel probe with a polished 413 µm wide tip (cleaned before each test with 100% ethanol on a Kimwipe®) was inserted through an articulated port in the chamber's side and aligned with a suspended droplet.

Acta Biomaterialia xxx (xxxx) xxx

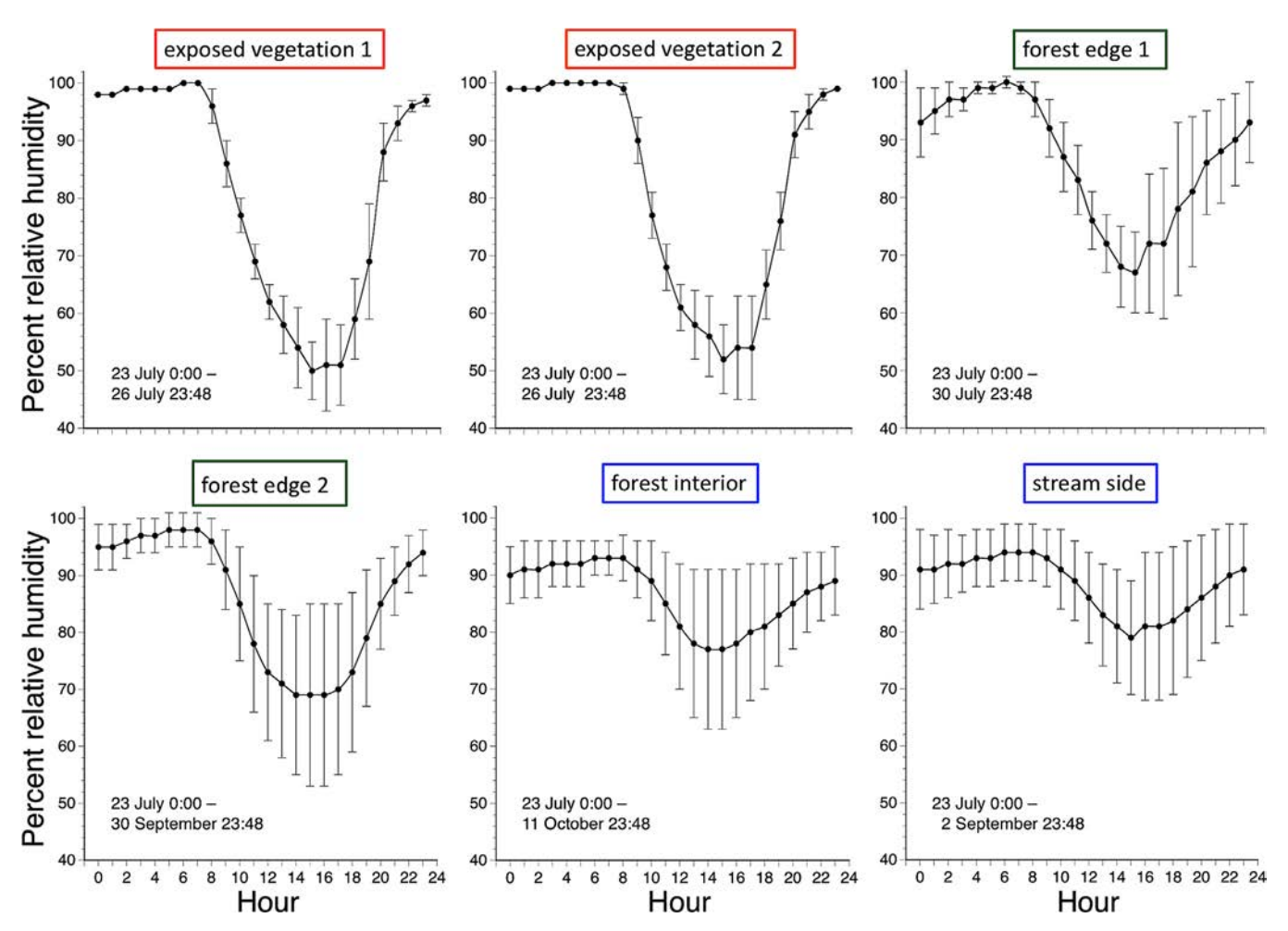


Fig. 4. Daily changes in relative humidity in low (orang), intermediate (green), and high (blue) humidity habitats where species included in this study were found. Each hour's value is the grand mean  $\pm$  1 standard deviation of values recorded by Onset HOBO U23 temperature and humidity data loggers (Boume, MA) at 12 minute intervals during the 2016 time periods indicated in the lower left of each plot.

After the shaft of the probe was locked into a stationary support, we advanced the mechanical stage's X axis 500  $\mu m$  to press the probe's tip against the droplet to securely adhere the droplet before engaging a stepping motor to move the X-axis in the opposite direction at 69.6  $\mu m~s^{-1}$ , extending the droplet while a 60-fps movie was captured.

#### 2.6. Computing extension per protein core volume

The droplets of some orb weaving species, particularly those with very hygroscopic droplets, transition from Phase 1 extension, during which the protein filament remains completely covered by aqueous material to Phase 2 extension, during which tiny drops of aqueous solution form on the filament, exposing unwetted regions of the protein filament [40,41]. Phase 1 performance corresponds to the performance of droplet during normal suspension bridge formation (Fig. 1E) [26] when its protein is fully hydrated and conditioned by the aqueous layer [16,25]. Therefore, we determined protein core properties only during Phase 1 extensions. We used an Onde Screen Ruler (OndeSoft, Minneapolis, MN) to measure a droplet's length just prior to pull-off or at the end of Phase 1 extension (Fig. 1E) and divided this length by the droplet's protein core volume to produce an extension per adhesive volume index as  $\mu m/\mu m^3$ .

# 2.7. Computing protein core elastic modulus and toughness at 55% RH

As described in a previous study [40], we used flagelliform fiber diameters and elastic moduli (taken from the literature for ten species [44] and newly determined for two species; Table S2) in conjunction with measurements of the angular deflection of a droplet's support line ( $\theta$  in Fig. 1E) and droplet length to constructed true stress - true strain curves (Fig. S1) and from these determined protein core elastic modulus and toughness. For T, elongate we used the flagelliform fiber values reported for T. versicolor [44]. Nano Bionix® instruments were used to determine these flagelliform fiber elastic modulus values (Table S2). These tests begin with a thread that is not under stress, allowing both the stress and strain axes of the resulting curve to originate at zero values. In the case of viscous capture threads, this opens the possibility that the windlass mechanism [45,46], which in some species is known to reel flagelliform fibers into a droplet when thread tension is reduced, operated during a test. In these cases a thread's stress - strain curve would include an initial, low stress phase during which these flagelliform fibers play out of the droplets before the fibers begin to extend. Following this, stress would increase as these fibers extend and enter a liner phase, during which their elastic modulus is characterized. This pattern was shown in the stress - strain curve of a species whose droplets exhibited the windlass mechanism (Movie S2 in [46]). Consequently, for species

Acta Biomaterialia xxx (xxxx) xxx

whose capture threads exhibited windlass flagelliform fiber reeling the resulting stress – strain curves would overestimate flagelliform fiber toughness. However, the elastic modulus of flagelliform fibers is determined during the linear, higher stress phase that occurs later in fiber extension. Therefore, we do not believe that the operation of a windlass mechanism compromised the determination of flagelliform fiber elastic modulus values that are used in this study.

As explained previously, the protein core of droplets that we characterized remained covered by their conditioning aqueous layers. Consequently, our methods do not allow us to distinguish the mechanical contributions of each component. However, given the substantial difference in viscosity of each component, we believe that these droplets' protein cores offered much greater resistance to extension than did their aqueous layers. This view is supported by the finding that the adhesive contribution of an orb weaver's protein core is two to three orders of magnitude greater than the capillary adhesion of its aqueous layer [2].

True stress – true strain curves were constructed from measurements taken at the initiation of a droplet's extension and at five intervals during its extension (Fig. S1). We established these intervals by divided the time between the initiation of droplet extension and droplet pull-off or the completion of Phase 1 extension into the 20% intervals. At the initiation of droplet extension and at each of these five positions we measured the angular deflection  $\theta$  of the droplet's support line (Fig. 1E) and at each of the five extension intervals also the length of the droplet filament. Tables S3-14 give support line angular deflections and droplet extensions at the initiation of droplet extension and at each 20% extension interval for each test RH.

After using the deflection of a droplet's support line to calculate the extension of the 2400µm long segment of line on either side of the droplet, we used the elastic modulus and diameters of the lines flagelliform fibers to determine the force this generated as a droplet extended. The lines' deflection angle was then used to resolve these force vectors and calculate the force on an extending droplet filament at each of the six extension intervals. We determined the true stress on a protein filament at each interval by dividing force on the droplet by protein cross sectional area (CSA). At the initiation of droplet extension we determined CSA as the diameter of the protein core when configured as a sphere (CoreDiam). At each of the following five intervals CSA was determined by dividing protein core volume by droplet length. We express the true strain on a droplet' protein filament as the natural log of droplet length divided by CoreDiam. The mean true stress and true strain values of all individuals of each species were plotted (Fig. S1) and from each species' plot the true strain range during which a slope was appropriate for determining elastic modulus was identified and subsequently used to calculate the elastic modulus of each individual's protein core material at 55% RH. Because a droplet was under stress when extension began, we subtracted the area of a thin rectangle defined by the initial true stress on a droplet and total droplet true strain from the total area under a true stress - true strain curve to determine protein core toughness.

We determined the force on extending protein filaments computationally rather than by direct measurement, as studies of orb weaver major ampullate radial and capture thread flagelliform fibers have done [44]. However, our construction of the true stress – true strain curves shown in Figure S1 and our determination of elastic modulus from these curves conforms to that of this and other studies [47-49]. Just as radial threads were much stiffer than capture thread support lines (grand means = 6.36 and 0.028 GPa, respectively), we anticipated that protein elastic modulus would be much less than that of the capture thread's flagelliform fibers. However, our determination of protein toughness differed in one way. Because a droplet was attached to the probe by its own ad-

hesion rather than being permanently affixed, when this adhesion failed the test ended, as did the true stress – true strain cures derived from it (Fig. S1). The shapes of these curves indicated that this did not affect our measurements of elastic modulus because the linear phase of true stress had either been established before droplet pull-off occurred or before phase 1 ended or because the stress on a filament had begun to decrease before measurements ended. However, as pull-off limits the protein's extension that might otherwise have been expressed, the value that we report as protein toughness might better be regarded as realized toughness, which is perhaps less than the protein core's inherent toughness.

#### 2.8. Inferring protein core elastic modulus at another test humidities

The procedures descried above appear reliable only for the 55% RH test interval because this is similar to the laboratory humidity at which flagelliform properties were determined. Not surprisingly, when a capture thread's aqueous layer is removed the thread's flagelliform fibers stiffen [50]. However, there are no published accounts of the response of coated flagelliform fibers to changes in humidity. A previous study that used the methods described above assumed that the stiffness of coated flagelliform fibers did not change with humidity [40], leading these authors to conclude that the stiffness of protein cores of two of the four orb weaving species studied increased as humidity increased. This is inconsistent with properties of a viscoelastic material that absorbs water, increase in volume, and become more pliable as humidity increases (Fig. 2; Tables S3 - S14). Therefore, we must conclude that flagelliform fibers contained within an aqueous layer respond to changes in humidity, although probably not to the same degree as do major ampullate fibers. Consequently, another method must be used to determine the material properties of orb web glue droplet core protein core at test humidities below and above the 55% RH test. Using a species' index of droplet extension per protein volume at 55% RH as a reference, we progressively increase protein elastic modulus values at humidities below 55% RH and proressively decreased elastic modulus values at humidites above 55% RH, resulting in a pattern of decreasing protein elatic modulus from 20% to 90% RH (Fig. 2).

To acomplish this we used one formula to infer protein core elastic modulus at humidities equal to and lower than that at which maximum extension per protein volume was registered (EMIL) and another to infer protein elastic modulus at humidities greater than that at which maximum extensoin per protein volume were registered (EMIH):

$$EMIL = EM55\% \times (EPV55\% \div EPVX\%)$$

$$EMIH = EM55\% \times (EPVX\% \div EPV55\%)$$

where EM55% = elastic modulus determined at 55%, EPV55% = extension per protein volume at 55% RH, and EPVX% = extension per protein volume at test humidity X. Inferred elastic modulus was determined relative to each individual's maximum extension per protein volume because a few individuals exhibited maximum extension per protein volume at humidities different from that typical of their species. When determined in this manner, the elastic modulus of V. arenata core protein at 20% and 37% relative humidity were very great (519 and 48 MPa, respectively). As we judged these values to be excessive, we modeled reported values on the increase in elastic modulus from 72% to 55% RH. We did this by dividing elastic modulus at 55% by 72% elastic modulus and multiplying this scaling factor by the 55% RH elastic modulus value to estimate 37% elastic modulus and by then multiplying this adjusted 37% RH elastic modulus value by the scaling factor to estimate elastic modulus at 20% RH. The standard errors of V. are-

Acta Biomaterialia xxx (xxxx) xxx

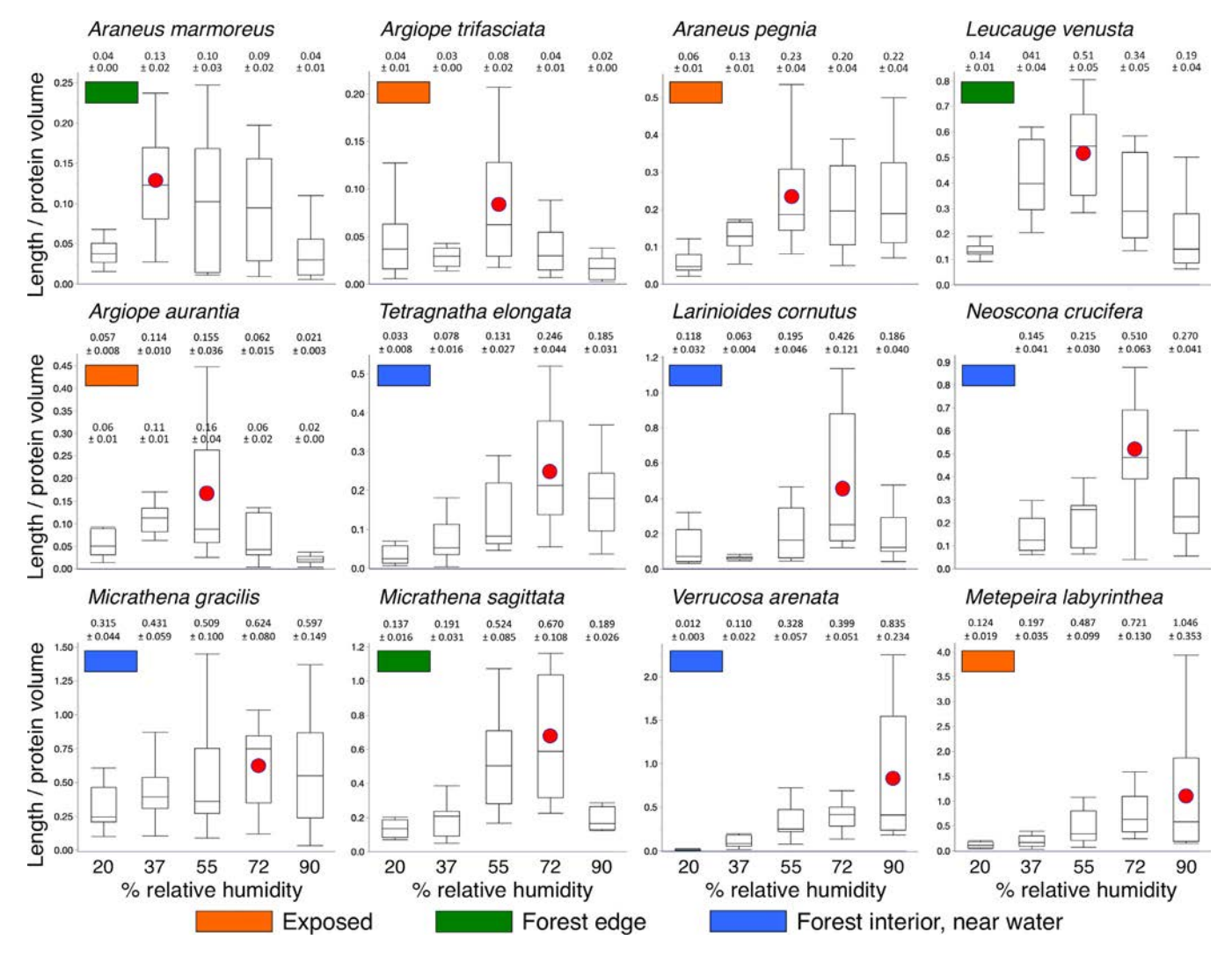


Fig. 5. Droplet extension lengths per protein core volume ( $\mu$ m/ $\mu$ m<sup>3</sup>), arranged in order of increasing humidity at which maximum values occur and identified by habitat humidity. The mean of each species' maximum value is marked with a red dot in its box plot. Values above each box are mean  $\pm$  1 standard error.

nata 20% and 37% RH elastic modulus are proportional to those that were initially determined.

## 2.9. Statistical analysis

We used JMP (SAS Institute, Cary, N.C.) to perform statistical analyses. Outliers, identified as any value less than (1.5 x the interquartile range) below the first quantile or more than (1.5 x the interquartile range) above the third quantile, were omitted before analyses were performed and values were plotted. Anderson-Darling tests for normal distribution of data showed that for all comparisons the means of one or more species or one or more humidity treatments within a species were not normally distributed (P < 0.05). Therefore, we used Wilcoxon / Kruskal-Wallis Chi Square tests and Wilcoxon each pair tests to compare means, considering differences with  $P \le 0.05$  to be significant. We ranked species according to the three habitat humidity categories shown in Fig. 3 and used contingency analyses to test the hypothesis that core protein properties were associated with habitat humidity, as supported by likelihood ratios P < 0.05.

## 3. Results

All high humidity species exhibited maximum extension per protein core volume at either 72 or 90% RH (Fig. 5). The edge

species M. sagittata exhibited maximum extension per core protein volume at 72% RH like its sister forest species M. gracilis, rather than at 55% RH, as did the edge species L. venusta. The two most notable deviations from this pattern were M. labyrinthea, a species that builds its webs on exposed vegetation and registered maximum extension per protein volume at 90% RH and A. marmoreus, a forest edge species and the only species to exhibit maximum extension per protein volume at 37% RH. When species were ordered by the humidity at which they expressed maximum extension per core protein volume and divided into four, three-species groups, a contingency analysis shows these groups to be associated with the three habitat humidity categories identified in Fig. 3 (likelihood ratio P = 0.0346).

Wilcoxon each pair ranking tests ordered the twelve species' core protein elastic modulus values at 55% RH into five groups (Fig. 6A) and their protein's toughness at 55% RH into three groups (Fig. 6B). However, neither property was associated with these species' habitat humidity rankings (contingency analysis likelihood ratio P = 0.1287 and 0.0922). Leucauge venusta, M. gracilis, and V. arenata proteins exhibited the greatest elastic modulus and toughness. Intra-specific differences in inferred protein elastic modulus across the 70% RH test range were considerable and differed greatly among species (Fig. 7). Not only was V. arenata protein the stiffest, but it also exhibited the greatest range of elastic modulus

JID: ACTBIO

Acta Biomaterialia xxx (xxxx) xxx

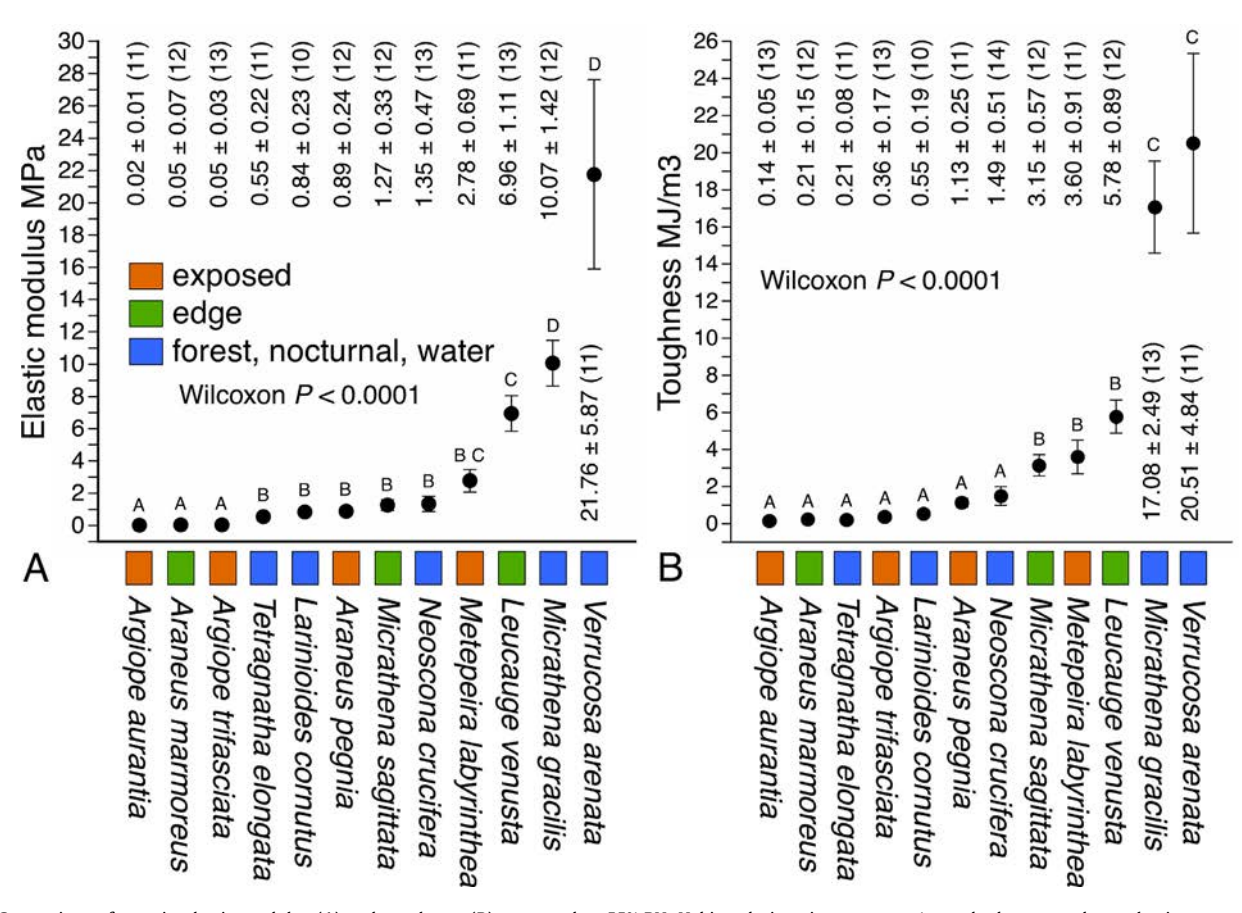


Fig. 6. Comparison of protein elastic modulus (A) and toughness (B) measured at 55% RH. Habitat designation, mean  $\pm$  1 standard error, and sample size are provided for each species. Wilcoxon *P* values are for comparisons of mean. Letters denote value rankings by Wilcoxon each pair tests.

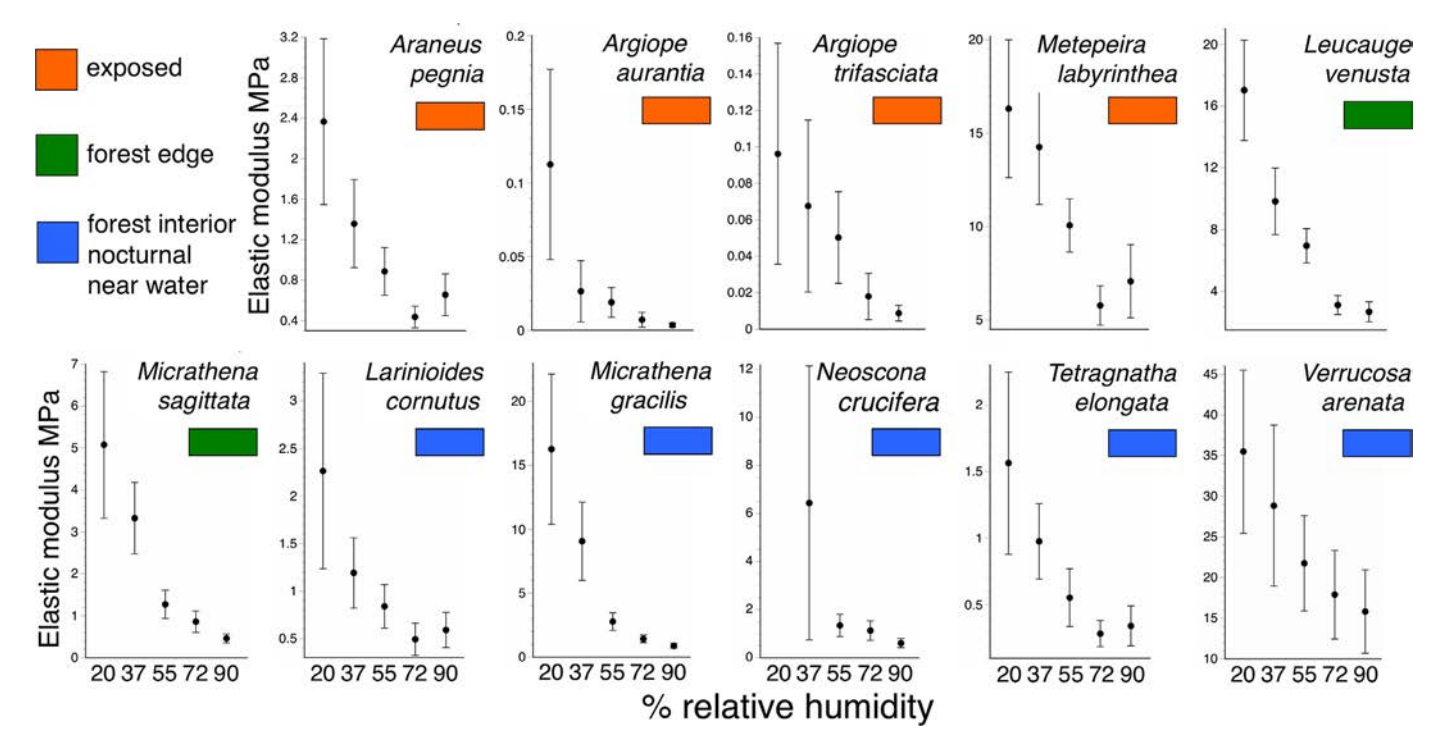


Fig. 7. Inferred protein core elastic modulus values at humidities below and above measured 55% RH values identified by species habitat humidity. Araneus marmoreus values are excluded because at all test humidities except 37% RH (mean  $0.09 \pm 0.10$  MPa) a high proportion of negative values occurred and were judged unreliable. Neoscona crucifera 20% RH values are not given because droplets of most individuals did not adhere at this humidity. Values are mean  $\pm$  1 standard error.

B.D. Opell, H.M. Elmore and M.L. Hendricks

Acta Biomaterialia xxx (xxxx) xxx

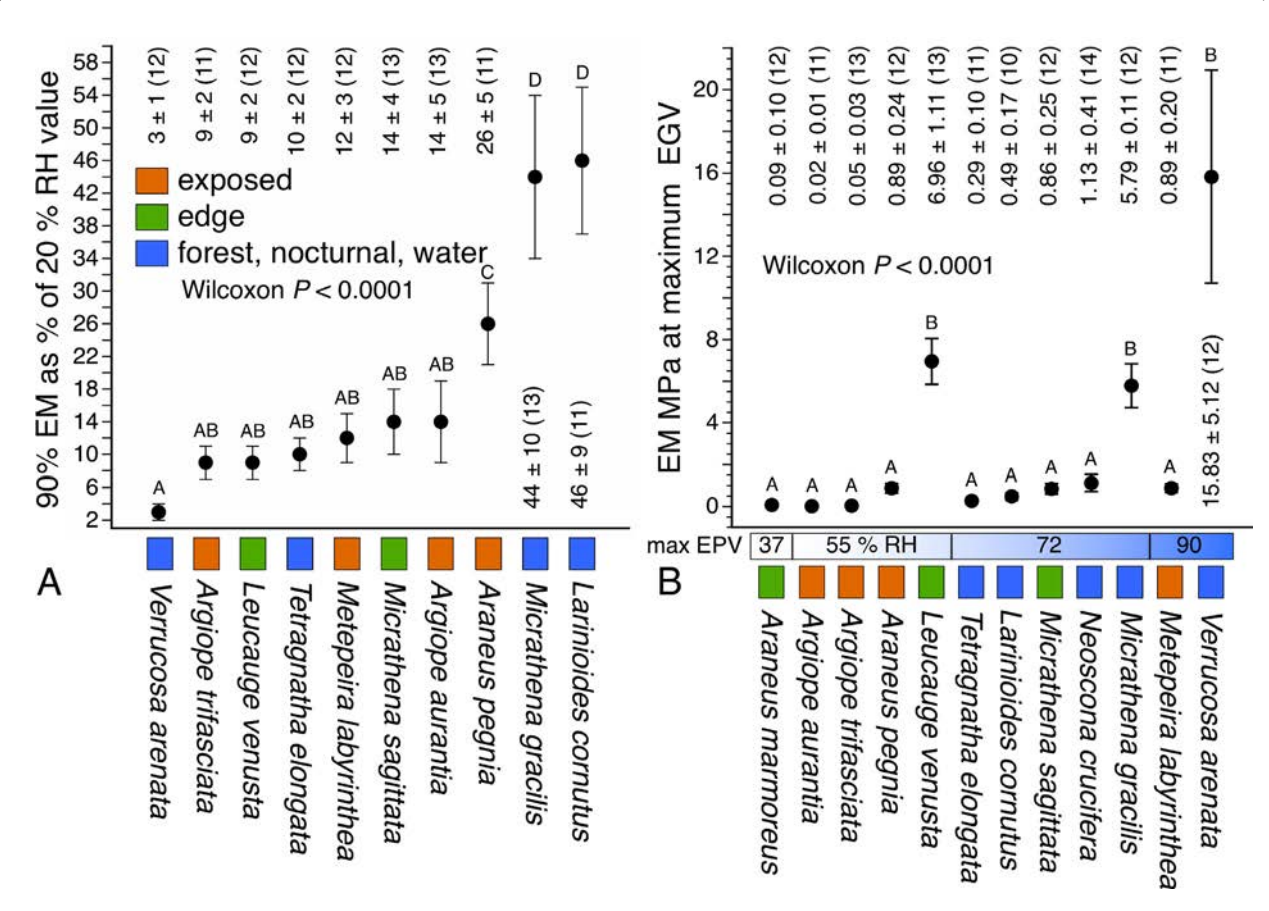


Fig. 8. Comparison of the percent reduction in inferred elastic modulus of core protein from 20% to 90% RH (A) and the measured or inferred elastic modulus at the RH for which maximum extension per protein volume (EPV) was observed (Fig. 4). Habitat designation, mean  $\pm$  1 standard error, and sample size are provided for each species. Wilcoxon *P* values are for comparisons of means. Letters denote value rankings by Wilcoxon each pair tests.

values, with its elastic modulus at 90% RH being only 3% of its 20% RH value (Fig. 8A). This contrasts with *L. cornutus* and *M. gracilis* proteins, whose 90% RH elastic modulus values averaged 45% of their 20% RH values.

The hypothesis that a species' core protein has been selected to perform optimally at its foraging humidity is most strongly supported by the similarity of protein elastic modulus values when compared at the humidity where each species' maximum extension per protein volume was observed (Fig. 8B). In contrast to 55% RH elastic modulus values, which comprise five groups (Fig. 6A), Wilcoxon each pair tests identified only two elastic modulus groups, with the proteins of L. venusta, M. gracilis, and V. arenata being much stiffer greater than those of other nine species. Moreover, the mean absolute difference of all pairwise comparisons of these twelve species' elastic modulus values at 55% RH was 5.92  $\pm$  0.85 MPa, but at the humidity of maximum extension per protein volume this difference decreased to 4.26  $\pm$  0.63 MPa (two-tailed, matched pairs test P < 0.0001), denoting a convergence in protein core stiffness. This convergence occurred across the species, as documented by the correlation of elastic modulus at maximum extension per protein volume (Y) and elastic modulus at 55% RH (X) (Y = 0.724 X - 0.023,  $R^2$  adjusted = 0.96, P <0.0001).

Our study was not intended to provide a phylogenetic assessment of glue droplet properties, as the tree we present is highly pruned and contains a small number of species (Fig. 3). However, we find little evidence that phylogenetic position plays a major role in the droplet properties that we observed. When arranged by the maximum true stress registered during droplet extension at 55% RH, the values of the two *Argiope* species were adjacent, as

were those of the two *Araneus* species (Fig. S1). These four species registered the lowest true stress, although four branch lengths separate the genera (Fig. 3). Neither 55% elastic modulus nor toughness values for *Araneus*, *Argiope*, and *Micrathena* species pairs were contiguous (Fig. 6). With the exception of percent decrease in elastic modulus with increased humidity (Fig. 8A), all values of the two Tetragnathidae species were interspersed among Araneidae species values.

#### 4. Discussion

In the course of testing the hypothesized association between droplet protein core properties and habitat humidity our study documented that, when surrounded by its conditioning aqueous layer, orb weaver core protein exhibits a remarkable range of material properties. At 55% RH these ranged from those of PEG-based hydrogels to those of silicone rubber, exhibiting a 1088-fold interspecific difference in stiffness (0.02 - 21.76 MPa) and a 147-fold difference in toughness (0.14 - 20.51 MJ/m³). Within a species, inferred elastic modulus decreased by 56 - 97% as humidity increased from 20 to 90% RH.

Results support the study's hypothesis that glue droplet properties are tuned to an orb weaving species' foraging humidity. As judged by extension per protein volume, the droplet performance of most species is optimized for humidities it encounters when foraging (Figs. 4 and 5). When measured at 55% RH, core protein elastic modulus also tends to increase with the humidity of a species' habitat (Fig. 6A), However, the most compelling support for this hypothesis comes from the observation that the elastic modulus values of species core proteins were more similar when compared

B.D. Opell, H.M. Elmore and M.L. Hendricks

Acta Biomaterialia xxx (xxxx) xxx

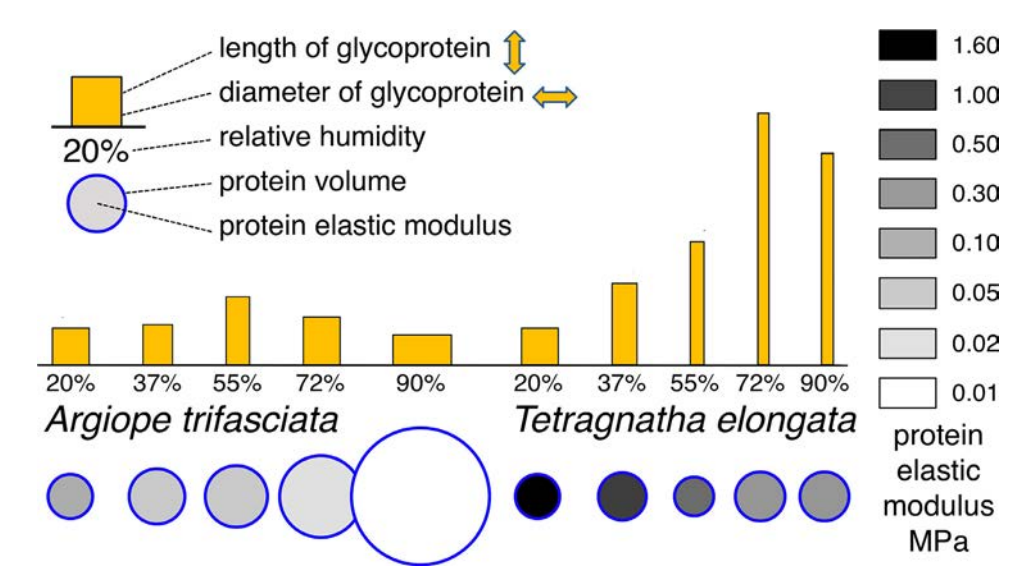


**Fig. 9.** Model of the impact of humidity on core protein volume, elastic modulus, and droplet extension of *A. aurantia*, a species with highly hygroscopic droplets that is found in exposed habitats, and *T. elongata*, a species with lesser hygroscopic droplets that is found near water. Dimensions of protein length, width, and volume are proportional to the values that each species expressed at 20% RH. Elastic modulus is proportional to the darkness of the volume's shading.

at the humidites of their maximum extension per protein volumes than when compared at 55% RH (cf. Figs. 6A and 8B). This is consistent with a previous study which found that, when measured at their foraging humidities, the viscosities of five species core proteins were remarkably similar [23]. This association, which appears to be driven by an inverse relationship between droplet hygroscopicity and a species' foraging humidity, ensures that the core proteins of species that construct webs on exposed vegetation remains pliable during hotter, drier parts of the day, whereas the proteins of species found in humid habitats resists over lubrication that would lead to adhesive failure.

The core proteins of *L. venusta*, *M. gracilis*, and *V. arenata* were distinguished both by greater elastic modulus and toughness at 55% RH (Fig. 6) and by greater elastic modulus at the humidity where maximum extension per protein volume occurred (Fig. 8B). There are no distinguishing similarities between the volumes of these species' protein cores at 55% RH (638, 1,886, 1,785 μm³ at 55% RH, respectively), their glue droplets per mm length of capture thread (29.9, 9.9, and 7.4, respectively) [26], or the space between capture thread spirals (2.5, 1.5, and 4.9 mm, respectively) [44]. However, of the species studied, *L. venusta*, *M. gracilis*, and *V. arenata* have the stiffest flagelliform fibers (58, 52, and 98 MPa, respectively). The stiffness of the other nine species ranged from 5 to 36 MPa and averaged 11 MPa (Table S2).

The greater stiffness of *V. arenat*a flagelliform fibers, has been associated with their playing a more important role in absorbing prey impact energy than is typical for orb weavers, where radial and frame lines usually dominate this role [6,51]. For example, the capture spirals of A. aurantia and A. trifasciata webs absorbed only 6% and 2%, respectively, as much energy as did their radial lines, whereas V. arenata capture spirals absorbed 83% as much energy as their webs' radial threads [6]. The greater stiffness of L. venusta and M. gracilis flagelliform fibers may also reflect an adaptation of these species' capture threads to absorb more prey impact energy than do the capture threads of the other species we studied. The stiffer and tougher protein cores of L. venusta, M. gracilis, and V. arenata capture threads would complement these thread's increased role in absorbing prey impact energy in two ways: 1. Stiffer protein would not extend as far during prey impact and would be less likely to rupture and 2. Tougher protein would absorb more energy as they extended. However, this would occur at a cost of reduced adhesive surface area of contact, which could limit thread adhesion to a prey. As *L. venusta* is the only species included in this study that constructs horizontal rather than vertical orb webs, it is surprising to see the stiffness of its core protein grouped with those of *M. gracilis* and *V. arenata*. However, the orientation of *L. venusta* webs and their typical placement nearer to the ground may exposes them to smaller forces of prey impact and, therefore, may have reduced selective for the energy absorbing roles of this species' radial and capture threads to diverge.

Natural selection tunes orb weaver glue droplet performance largely by altering the composition and concentration of LMMCs in the droplet's aqueous layer, although core protein also appears to contribute to droplet hygroscopicity [16,17,23,25]. The effect of this can be seen by comparing the humidity responses of A. trifasciata, whose droplets perform optimally at 55% RH, with those of T. elongata, whose droplets perform optimally at 72% RH (Fig. 9). As humidity increases, protein cores within the more hygroscopic droplets of A. trifasciata, swell, causing the elastic modulus of this protein to drop until an optimal balance between the surface area of adhesive contact at the droplet's footprint and the cohesion of the extending protein filament is achieved at 55% RH. As humidity continues to increase protein elastic modulus falls and protein filaments pull off at shorter extensions, despite their increasing areas of adhesive contact. In contrast, T. elongata droplets are less hygroscopic, causing their protein cores to reach optimal elastic modulus values only at 72% RH and to begin to become over lubricated only

The approach we used to infer elastic modulus below and above 55% RH of humidity allowed us to extend our calculated values and use these to test the study's hypothesis. However, this approach does have limitations. Droplet extension length is determined not only by core protein volume and elastic modulus, but also by both the area of a droplet's core protein contact and the strength of its adhesion. The interplay between these factors is complex and their relative contributions to droplet extension length may change with humidity. Indices of core protein viscosity that gauge a droplet ability to establish adhesive contact were calculated from the velocity of droplet spread during the milliseconds following droplet contact [23], whereas elastic modulus is an index of the energy required to extend a given volume of material and, in our study, was determined over longer time spans.

Acta Biomaterialia xxx (xxxx) xxx

## 5. Conclusions

An orb web's architectural, biomechanical, and chemical complexity provides many components and levels on which natural selection can operate to optimize web performance. The substantial uncoupling of the web's prey stopping and prey retention functions in most species frees viscous capture threads to evolve adhesion tailored to a species' foraging humidity. We observed this in extension per core protein volume, which tended to peak at lower humidities in species that occupy exposed, low humidity habitats, and at higher humidities in nocturnal species and those found in humid habitats. The tendency for the droplet hygroscopicity of a species' glue droplets to be inversely related to its foraging humidity helps ensure that core protein stiffness will be appropriate for the species' foraging humidity; neither too great for the dryer conditions experienced by orb weavers that live in exposed habitats nor too small for species that live in humid habitats. This explains why, when compared at humidities where maximum extension per protein volume was expressed, the elastic modulus of most species were more similar than they were at 55% RH. The biomimetic potential of orb spider capture threads has receiving some attention [46,52], however not nearly as much as the web's major ampullate threads [53,54]. By profiling the humidity responsiveness and properties of these spiders' glue droplets our study adds to the awareness of how this natural adhesive operates.

#### **Declaration of Competing Interest**

The authors declare no conflict of interest.

#### Acknowledgments

Sheree Andrews, Mary Clouse, Sarah Helweg, Kea Kiser, and Sarah Stellwagen assisted with droplet testing and measured suspended glue droplets. Sandra Correa-Garhwal characterized the elastic modulus of *Araneus pegnia* and *Micrathena sagittata* flagelliform fibers.

#### **Funding**

National Science Foundation grants IOS-1257719 and IOS-1755028 supported this study.

## **Authors' contributions**

BDO developed the instrumentation used to characterize droplet features, collected thread samples and prepared droplets for extension, supervised and participated in droplet testing, established the workflow and formulas for determining protein material properties, conducted statistical analyses, prepared figures and wrote the manuscript. HME assisted in setting up the JMP spreadsheet used to calculate material properties, measured droplet extension movies, and prepared summary tables of droplet features used in stress-strain curves. MLH measured the features of flattened glue droplets and computed protein volumes.

## Supplementary materials

Supplementary material associated with this article can be found, in the online version, at doi:10.1016/j.actbio.2021.06.017.

#### References

- [1] J. van der Gucht, Grand challenges in soft matter physics, Front. Phys. 6 (2018) 67.
- [2] V. Sahni, T.A. Blackledge, A. Dhinojwala, Viscoelastic solids explain spider web stickiness, Nat. Commun. 1 (19) (2010) 1–4, doi:10.1038/ncomms1019.

- [3] F. Vollrath, E.K. Tillinghast, Glycoprotein glue beneath a spider web's aqueous coat. Naturwissenschaften 78 (1991) 557–559.
- [4] J.E. Garb, N.A. Ayoub, C.Y. Hayashi, Untangling spider silk evolution with spidroin terminal domains, BMC Evol. Biol. 10 (2010) 243.
- [5] M.A. Collin, T.H. Clarke, N.A. Ayoub, C.Y. Hayashi, Evidence from multiple species that spider silk glue component ASG2 is a spidroin, Sci. Rep. 6 (2016) 21589
- [6] A. Sensenig, K.A. Lorentz, S.P. Kelly, T.A. Blackledge, Spider orb webs rely on radial threads to absorb prey energy, Interface 9 (2012) 1880–1891.
- [7] S.P. Kelly, A. Sensenig, K.A. Lorentz, T.A. Blackledge, Damping capacity is evolutionarily conserved in the radial silk of orb-weaving spiders, Zoology 114 (2011) 233–238.
- [8] W.G. Eberhard, Function and phylogeny of spider webs, Annu. Rev. Ecol. Systematics 21 (1990) 341–372.
- [9] J.A. Coddington, Spinneret silk spigot morphology: Evidence for the monophyly of orb-weaving spiders, Cyrtophorinae (Araneidae), and the group Theridiidae plus Nesticidae, J. Arachnol. 17 (1989) 71–96.
- [10] K. Sekiguchi, On a new spinning gland found in geometric spiders and its function, Annotationes Zoologicae Japonenses 25 (1952) 394–399.
- [11] H.M. Peters, Über den spinnapparat von Nephila madagascariensis, Zeitschrift für Naturforschung 10 (1955) 395–404.
- [12] D. Edmonds, F. Vollrath, The contribution of atmospheric water vapour to the formation and efficiency of a spider's web, Proc. R. Soc. Lond. 248 (1992) 145–148.
- [13] F. Vollrath, W.J. Fairbrother, R.J.P. Williams, E.K. Tillinghast, D.T. Bernstein, K.S. Gallagher, M.A. Townley, Compounds in the droplets of the orb spider's viscid spiral, Nature 345 (1990) 526–528.
- [14] N.A. Ayoub, K. Friend, T. Clarke, R. Baker, S. Correa-Garhwal, A. Crean, E. Dendev, D. Foster, L. Hoff, S.D. Kelly, W. Patterson, C.Y. Hayashi, B.D. Opell, Protein composition and associated material properties of cobweb spiders' gumfoot glue droplets, Integr. Comp. Biol. (2021) in press.
- [15] G. Amarpuri, V. Chaurasia, D. Jain, T.A. Blackledge, A. Dhinojwala, Ubiquitous distribution of salts and proteins in spider glue enhances spider silk adhesion, Sci. Rep. 5 (9053) (2015) 1–7.
- [16] D. Jain, G. Amarpuri, J. Fitch, T.A. Blackledge, A. Dhinojwala, Role of hygroscopic low molecular mass compounds in responsive adhesion of spiders capture silk, Biomacromolecules 19 (2018) 3048–3057.
- [17] M.A. Townley, E.K. Tillinghast, Aggregate Silk Gland Secretions of Araneoid Spiders, in: W. Nentwig (Ed.), Spider Ecophysiology, Springer-Verlag, New York, 2013, pp. 283–302.
- [18] G. Amarpuri, C. Zhang, T.A. Blackledge, A. Dhinojwala, Adhesion modulation using glue droplet spreading in spider capture silk, J. R. Soc. Interface 14 (2017) 20170228.
- [19] D. Jain, C. Zhang, L.R. Cool, T.A. Blackledge, C. Wesdemiotis, T. Miyoshi, A. Dhinojwala, Composition and function of spider glues maintained during the evolution of cobwebs, Biomacromolecules 16 (2015) 3373–3380.
- [20] G.V. Guinea, M. Cerdeira, G.R. Plaza, M. Elices, J. Pe fez-Rigueiro, Recovery in viscid line fibers, Biomacromolecules 11 (2010) 1174–1179.
- [21] V. Sahni, T. Miyoshi, K. Chen, D. Jain, S.J. Blamires, T.A. Black-ledge, A. Dhinojwala, Direct solvation of glycoproteins by salts in spider silk glues enhances adhesion and helps to explain the evolution of modern spider orb webs, Biomacromolecules 15 (2014) 1225–1232.
- [22] M.A. Townley, D.T. Bernstein, K.S. Gallagher, E.K. Tillinghast, Comparative study of orb web hygroscopicity and adhesive spiral composition in three araneid spiders, J. Exp. Zool. 259 (1991) 154–165.
- [23] G. Amarpuri, C. Zhang, C. Diaz, B.D. Opell, T.A. Blackledge, A. Dhinojwala, Spiders tune glue viscosity to maximize adhesion, ASC Nano 9 (2015) 11472–11478.
- [24] S.D. Kelly, B.D. Opell, L.L. Owens, Orb weaver glycoprotein is a smart biological material, capable of repeated adhesion cycles, Sci. Nature 106 (2019) 10.
- [25] B.D. Opell, D. Jain, A. Dhinojwala, T.A. Blackledge, Tuning orb spider glycoprotein glue performance to habitat humidity, J. Exp. Biol. 221 (2018) 1–12.
- [26] B.D. Opell, M.L. Hendricks, The adhesive delivery system of viscous prey capture threads spin by orb-weaving spiders, J. Exp. Biol. 212 (2009) 3026–3034.
- [27] Y. Guo, Y. Chang, H. Guo, W. Fang, Q. Li, H. Zhao, X. Feng, H. Gao, Synergistic adhesion mechanisms of spider capture silk, Interface 15 (2018) 20170894.
- [28] Y. Guo, H. Zhao, X. Feng, H. Gao, On the robustness of spider capture silk's adhesion, Extreme Mech. Lett. 29 (2019) 100477.
- [29] V. Sahni, T.A. Blackledge, A. Dhinojwala, Changes in the adhesive properties of spider aggregate glue during the evolution of cobwebs, Sci. Rep. 1 (41) (2011) 1–8.
- [30] R.J. Stewart, T.C. Ransom, V. Hlady, Natural underwater adhesives, J. Polym. Sci. Part B Polymer Phys. 49 (2011) 757–771.
- [31] World Spider Catalog, World Spider Catalog v21.5. 2020 (accessed August 26, 2020).
- [32] J.E. Bond, B.D. Opell, Testing adaptive radiation and key innovation hypotheses in spiders, Evolution 52 (1998) 403–414.
- [33] W.G. Eberhard, I. Agnarsson, H.W. Levi, Web forms and phylogeny of theridiid spiders (Araneae: Theridiidae), Syst. Biodivers. 6 (2008) 415–475.
- [34] S. Benjamin, S. Zschokke, Homology behaviour and spider webs: web construction behaviour of Linyphia hortensis and L. triangularis (Araneae: Linyphiidae) and its evolutionary significance, J. Evol. Biol. 17 (2004) 120–130.
- [35] W.G. Eberhard, Spider webs: function, behavior and evolution, University of Chicago Press, Chicago, 2020.

## ARTICLE IN PRESS

JID: ACTBIO [m5G; July 3, 2021;15:15]

B.D. Opell, H.M. Elmore and M.L. Hendricks

Acta Biomaterialia xxx (xxxx) xxx

- [36] H.M. Peters, J. Kovoor, The silk-producing system of Linyphia triangularis (Araneae, Linyphiidae) and some comparisons with Araneidae. Structure, histochemistry and function, Zoomorphology 111 (1991) 1–17.
- [37] B.D. Opell, S.E. Karinshak, M.A. Sigler, Environmental response and adaptation of glycoprotein glue within the droplets of viscous prey capture threads from araneoid spider orb-webs, J. Exp. Biol. 216 (2013) 3023–3034.
   [38] B.D. Opell, C.M. Burba, P.D. Deva, M.H.Y. Kin, M.X. Rivas, H.M. Elmore,
- [38] B.D. Opell, C.M. Burba, P.D. Deva, M.H.Y. Kin, M.X. Rivas, H.M. Elmore, M.L. Hendricks, Linking properties of an orb weaving spider's capture thread glycoprotein adhesive and flagelliform fiber components to prey retention time, Ecol. Evol. 2019 (2019) 1–14.
- [39] D. Dimitrov, L.R. Benavides, M.A. Arnedo, G. Giribet, C.E. Griswold, N. Scharff, G. Hormiga, Rounding up the usual suspects: a standard target-gene approach for resolving the interfamilial phylogenetic relationships of ecribellate orb-weaving spiders with a new family-rank classification (Araneae, Araneoidea), Cladistics 33 (2017) 221–250.
- [40] B.D. Opell, M.E. Clouse, S.F. Andrews, Elastic modulus and toughness of orb spider glycoprotein glue, PLoS One 13 (5) (2018) e0196972 21 pages.
- [41] B.D. Opell, S.D. Stellwagen, Properties of orb weaving spider glycoprotein glue change during *Argiope trifasciata* web construction, Sci. Rep. 9 (2019) 20279.
- [42] Image J. http://www.uhnresearch.ca/facilities/wcif/imagej/, Bethesda, Maryland, U.S.A., 2006.
- [43] C. Liao, S.J. Blamires, M.L. Hendricks, B.D. Opell, A re-evaluation of the formula to estimate the volume of orb web glue droplets, J. Arachnol. 43 (2015) 97–100.
- [44] A. Sensenig, I. Agnarsson, T.A. Blackledge, Behavioral and biomaterial coevolution in spider orb webs, J. Evol. Biol. 23 (2010) 1839–1856.

- [45] H. Elettro, S. Neukirch, V. F., A. Antkowiak, In-drop capillary spooling of spider capture thread inspires hybrid fibers with mixed solid-liquid mechanical properties, Proc. Natl. Acad. Sci. 22 (2016) 6143–4617.
- [46] H. Elettro, F. Vollrath, S. Neukirch, A. Antkowiak, In-drop capillary spooling of spider capture thread inspires hybrid fibers with mixed solid-liquid mechanical properties, Proc. Natl. Acad. Sci. 113 (2016) 6143–6147.
   [47] T.A. Blackledge, C.Y. Hayashi, Silken toolkits: biomechanics of silk fibers spun
- [47] T.A. Blackledge, C.Y. Hayashi, Silken toolkits: biomechanics of silk fibers spun by the orb web spider Argiope argentata (Fabricius 1775), J. Exp. Biol. 209 (2006) 2452–2461.
- [48] T.A. Blackledge, C.Y. Hayashi, Unraveling the mechanical properties of composite silk threads spun by cribellate orbweaving spiders, J. Exp. Biol. 209 (2006) 3131–3140.
- [49] B.O. Swanson, T.A. Blackledge, J. Beltrán, C.Y. Hayashi, Variation in the material properties of spider dragline silk across species, Appl. Phys. A Mater. Sci. Process. 82 (2006) 213–218.
- [50] G.V. Guinea, M. Cerdeira, G.R. Plaza, M. Elices, J. Pérez-Rigueiro, Recovery in Viscid Line Fibers, Biomacromolecules 11 (2010) 1174–1179.
- [51] A. Sensenig, S.P. Kelly, K.A. Lorentz, B. Lesher, T.A. Blackledge, Mechanical performance of spider orb webs is tuned for high-speed prey, J. Exp. Biol. 216 (2013) 3388–3394.
- [52] V. Sahni, D.V. Labhasetwar, A. Dhinojwala, Spider silk inspired functional microthreads, Langmuir 28 (2012) 2206–2210.
- [53] F. Vollrath, The complexity of silk under the spotlight of synthetic biology, Biochem. Soc. Trans. 44 (2016) 1151–1157.
- [54] F. Vollrath, D. Porter, Spider silk as a model biomaterial, Appl. Phys. A 82 (2006) 205–212.